Protostane Triterpenoids from the Rhizome of Alisma orientale Exhibit Inhibitory Effects on Human Carboxylesterase 2

ARTICLE *in* JOURNAL OF NATURAL PRODUCTS · OCTOBER 2015

Impact Factor: 3.8 · DOI: 10.1021/acs.jnatprod.5b00321

JOURNAL OF NATURAL PRODUCTS

Article

pubs.acs.org/jnp

Protostane Triterpenoids from the Rhizome of *Alisma orientale* Exhibit Inhibitory Effects on Human Carboxylesterase 2

Zhen-Peng Mai,[†] Kun Zhou,[‡] Guang-Bo Ge,[§] Chao Wang,*[,†,∥] Xiao-Kui Huo,[†] Pei-Pei Dong,[†] Sa Deng,[†] Bao-Jing Zhang,[†] Hou-Li Zhang,[†] Shan-Shan Huang,[†] and Xiao-Chi Ma*[,†,∥]

[†]College of Pharmacy, Key Laboratory of Metabolism and Transport of Liaoning, and [∥]Liaoning Province Key Laboratory of Natural Products for Neurodegenerative Diseases, Dalian Medical University, Dalian 116044, People's Republic of China

[‡]College of Pharmacy, Liaoning University of Traditional Chinese Medicine, Dalian 110847, People's Republic of China

[§]Laboratory of Pharmaceutical Resource Discovery, Dalian Institute of Chemical Physics, Chinese Academy of Sciences, Dalian 116023, People's Republic of China

Supporting Information

ABSTRACT: Twelve new and 10 known protostane triterpenoids were isolated from the rhizome of *Alisma orientale*. Their structures were elucidated based on physical data analyses, including UV, HRESIMS, NMR experiments (^{1}H, ^{13}C NMR, ^{1}H−^{1}H COSY, HSQC, HMBC, and NOESY), and induced electronic circular dichroism. New compounds **1**−**12** were classified as protostanes (**1**−**10**), 29-norprotostane (**11**), and 24-norprotostane (**12**) by structure analyses. Furthermore, the inhibitory effects on human carboxylesterases (hCE-1, hCE-2) of compounds **1**−**22** were evaluated. Compounds **2**, **6**, **9**, and **11** showed moderate inhibitory activities and were selective toward hCE-2 enzymes, with IC_{50} values of 8.68, 4.72, 4.58, and 2.02 μM, respectively. The inhibition kinetics of compound **11** toward hCE-2 were established, and the K_i value was determined as 1.76 μM using a mixed inhibition model. The interaction of bioactive compound **11** with hCE-2 was shown using molecular docking.

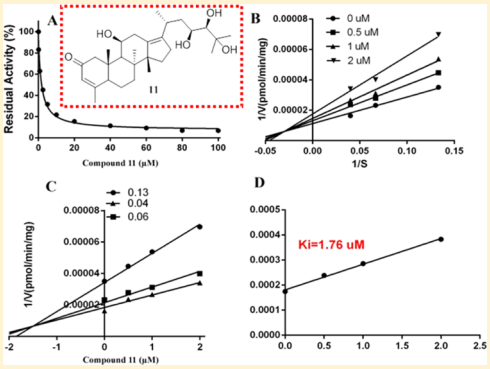

Alisma orientale (Sam.) Juz. (Alismataceae) is an aquatic plant that is widely distributed in China, Japan, North America, and Europe. The dried rhizome is a well-known traditional Chinese medicine (*R. Alismatis* or *Zexie*), which is classified into two types—*Jian Zexie* (*R. Alismatis* from the Fujian Province, China) and *Chuan Zexie* (*R. Alismatis* from the Sichuan Province, China)—based on their region of origin. This Chinese crude drug is also widely used in Japan. It has been used as a diuretic and as a folk medicine for diabetes in traditional Chinese medicine, and it is an important component of several Chinese preparations. Previous chemical investigations of *R. Alismatis* revealed the presence of polysaccharides,[1] guaiane-type sesquiterpenoids,[2] kaurane-type diterpenoids,[3] and protostane-type triterpenoids.[4] Protostane triterpenoids are the primary components of this plant, and they possess diuretic, hypopietic, hypolipemic, and antiatherosclerotic activities.[4a,5] Additionally, the significant hypoglycemic activity of compounds from *R. Alismatis* may be deduced via the inhibition of α-glucosidase activity and promotion of glucose uptake.[6] Bioassays have also indicated that protostane triterpenoids have potential inhibitory effects on vascular contraction,[7] immunosuppressive effects,[8] and anti-HBV effects.[9] Therefore, protostane triterpenoids may be important resources for the development of drugs and functional foods.

Human carboxylesterases hCE-1 and hCE-2 are important and highly homologous enzymes.[10] The hCE-1 enzyme is highly expressed in the liver and has beneficial effects on lipid and carbohydrate metabolism,[11] whereas the loss of hepatic hCE-1 due to chemical inhibition typically results in a fatty liver and a pro-atherogenic lipid profile. The hCE-2 enzyme is highly expressed in the intestine and catalyzes the hydrolysis of esters, amides, thioesters, and carbamates. Therefore, hCE-2 is a major mediator of drug metabolism that enhances drug bioavailability and reduces drug toxicity. Recently, a specific inhibitor of hCE-2 that does not affect hCE-1 and is derived from natural products has attracted attention.[12]

Owing to the high content of protostane triterpenoids in *A. orientale*, we elected to study the analogues from the rhizoma of *A. orientale* that have inhibitory effects on hCE-1 and hCE-2. A combination of chromatographic techniques led to the isolation of 22 protostane triterpenoids (**1**−**22**), including new protostanes (**1**−**10**), 29-norprotostane (**11**), and 24-norprotostane (**12**), the structures of which were elucidated by various physical methods, including 1D and 2D NMR, HRESIMS, and induced electronic circular dichroism (IECD). In a bioassay of compounds **1**−**22**, compounds **2**, **6**, **9**, and **11** showed moderate inhibitory activities against hCE-2, with IC_{50} values of 8.68, 4.72, 4.58, and 2.02 μM, respectively. None of the

Received: April 11, 2015

DOI: 10.1021/acs.jnatprod.5b00321
J. Nat. Prod. XXXX, XXX, XXX−XXX

Chart 1

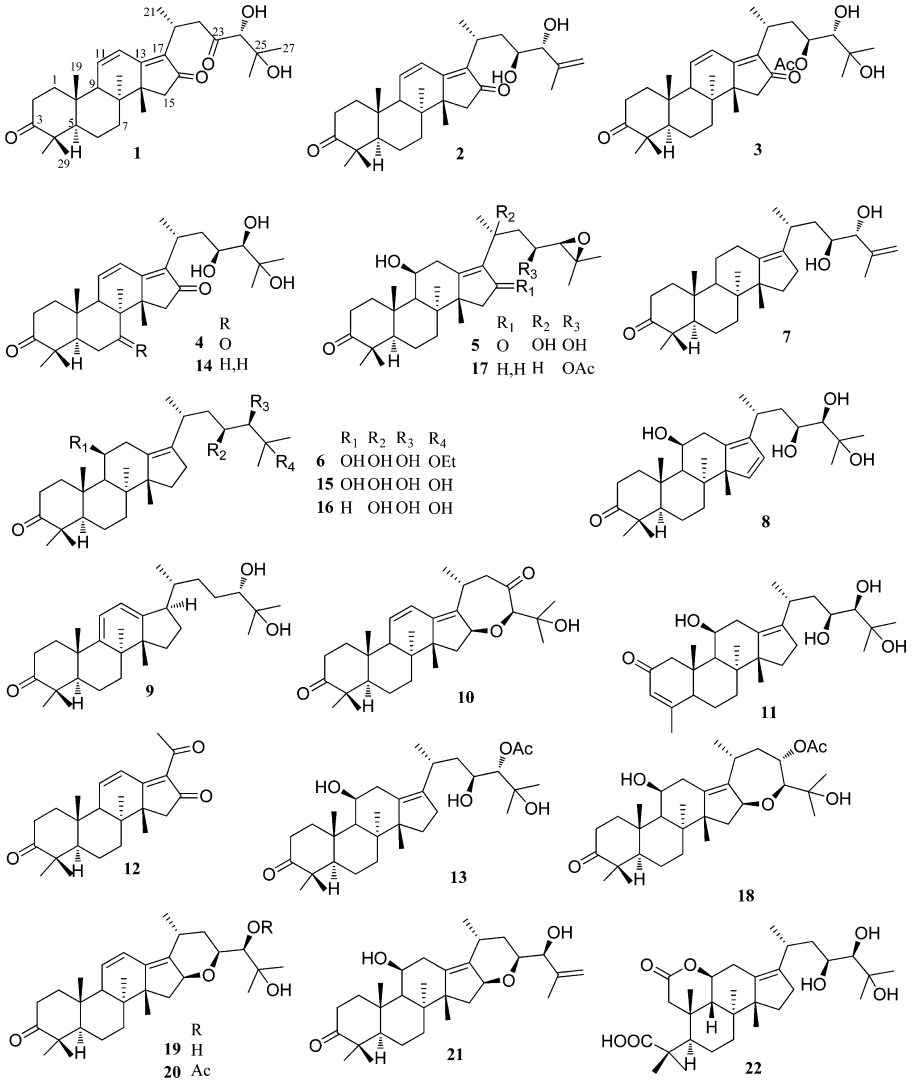

compounds inhibited hCE-1. Additionally, the interaction mechanism between hCE-2 and compound **11** was analyzed by a molecular docking study.

RESULTS AND DISCUSSION

Compound **1** was obtained as a white, amorphous powder. The molecular formula was established from the ^{13}C NMR data and a sodium adduct ion at m/z 507.3085 $[M + Na]^+$ (calculated for $C_{30}H_{44}NaO_5$, 507.3081) in the positive HRESIMS mode. The UV spectrum displayed the absorption of a conjugated dienone moiety at 289 nm.

The dienone moiety was also deduced from the ^1H NMR and ^{13}C NMR data [δ_H 6.86 (dd, J = 10.5, 2.0 Hz), 6.38 (dd, J = 10.5, 3.0 Hz); δ_C 210.2, 173.1, 140.1, 140.0, and 123.3]. The ^1H NMR spectrum displayed the presence of an oxygenated methine [δ_H 3.85 (s)], five tertiary methyls [δ_H 1.17, 1.16, 1.11, 1.04, 1.02 (each 3H, s)], three secondary methyl groups [δ_H 1.19 d (J = 7.0 Hz), 1.25, 1.16 (each 3H, s)], and an isolated methylene adjacent to a carbonyl carbon [δ_H 2.44 d (J = 18.5 Hz), 1.95 d (J = 18.5 Hz)]. The ^{13}C NMR spectrum revealed 30 carbons, which confirmed the above-mentioned moieties and suggested the presence of two isolated carbonyl carbons (δ_C 222.3, 213.7) and an additional oxygenated carbon (δ_C 73.2). Analyses of the physical data suggested that compound **1** was a protostane-type triterpenoid similar to alisol L 23-acetate isolated from *A. orientale*.[3] The long-range correlations [δ_C 222.3/H-28 (δ_H 1.16), H-29 (δ_H 1.11)] observed in the HMBC spectrum indicated the presence of a 3-carbonyl group (Figure 1). The position of the dienone moiety was established at C-11−C-12−C-13−C-17−C-16 by the long-range correlations of H-11/C-9, H-12/C-13, H-12/C-17, and H-15/C-16. Compared with alisol L 23-acetate, some differences were observed in the structure of the C-17 side chain. The oxygenated carbons (C-24, C-25) and carbonyl carbon (C-23) were established for the side chain based on the HMBC correlations of C-25 (δ_C

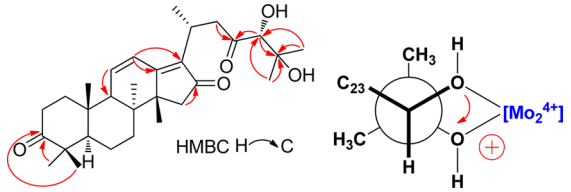

Figure 1. Key HMBC correlations and preferred conformation of the 24,25-diol moiety in the chiral Mo complex of compound **1**.

DOI: 10.1021/acs.jnatprod.5b00321
J. Nat. Prod. XXXX, XXX, XXX−XXX

73.2)/H-24, H-26, H-27; C-24 (δ_C 83.7)/H-26, H-27; and C-23 (δ_C 213.7)/H-22, H-24.

The absolute configurations of the stereogenic centers of the protostane skeleton were previously reported.[13] The absolute configuration of C-24 was determined via the $Mo_2(OAc)_4$-induced ECD method developed by Snatzke.[14] The positive Cotton effect at 305.5 nm indicated a 24*R* configuration (Figures 1 and 2). Accordingly, the structure of compound **1** was elucidated, as shown in Figure 1, and the compound was named alismanol A.

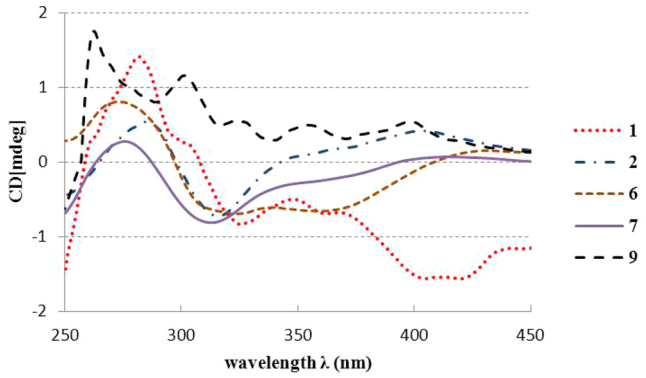

Figure 2. $Mo_2(OAc)_4$-induced ECD spectra of compounds **1**, **2**, **6**, **7**, and **9**.

Compound **2** was assigned the molecular formula $C_{30}H_{44}O_4$ by the HRESIMS and NMR data (Tables 1 and 2). A conjugated dienone moiety was deduced by the UV absorption at 290 nm. Analyses of the ^1H and ^{13}C NMR spectroscopic data revealed structural similarities to compound **1** and alisol L 23-acetate,[2b,3a] with the differences residing in the side chain. The ^1H and ^{13}C NMR data indicated two oxygenated methines [δ_H 3.71 (d, J = 7.0 Hz), 3.23 (m); δ_C 72.2, 81.3] and one terminal olefinic methylene group [δ_H 4.92 (m), 4.86 (m); δ_C 146.5, 113.9] in the side chain of **2**. The HMBC correlations of H-26 (δ_H 4.86)/C-27 (δ_C 18.1), H-24 (δ_H 3.71)/C-27 (δ_C 18.1), C-25 (δ_C 146.5), and H-23 (δ_H 3.23)/C-20 (δ_C 27.2), C-24 (δ_C 81.3) established the structure of the C-17 side chain. A *threo* 23,24-diol group could be deduced from the doublet of H-24 (d, J = 7.0 Hz) in the ^1H NMR spectrum. The negative Cotton effect at 310 nm in the IECD spectrum established the 23*S*, 24*R* configurations (Figure 2).[13] Thus, the structure of alismanol B (**2**) was assigned as shown.

Compound **3** possessed a molecular formula of $C_{32}H_{48}O_6$ as determined by the ^{13}C NMR and HRESIMS data (m/z 551.3352 $[M + Na]^+$; calcd $C_{32}H_{48}NaO_6$, 551.3343). The ^1H and ^{13}C NMR data of **3** (Tables 1 and 2) displayed resonances typical of a protostane-type triterpenoid. The 3-carbonyl group was determined by the correlations of C-3 (δ_C 222.3)/H-28 (δ_H 1.19), H-29 (δ_H 1.16). The location of the dienone group was assigned at C-11−C-12−C-13−C-16−C-17 based on the HMBC correlations. The 24,25-dihydroxy substituents in the side chain of **3** were established by the 1D and 2D NMR data. Additionally, one acetoxy group was located at 23-OH based on the HMBC correlation of H-23 (δ_H 4.83)/Ac carbonyl (δ_C 172.5). The doublet of H-24 (J = 7.0 Hz) observed in the ^1H NMR spectrum indicated the *threo* 23-OAc, 24-OH configuration. Makabel and co-workers reported the intramolecular transacetylation of alisol A 24-acetate.[15] Moreover, both alisol A 24-acetate and 23-acetate are susceptible to deacetylation into alisol A when stored in methanol for a long time.[14] The *threo* 23-OAc, 24-OH configuration in compound **3** corresponded to a stable structure without the transfer of an acetyl group from 23-OH to 24-OH. On the basis of the 20*R* configuration in protostane triterpenoids isolated from *A. orientale* and the correlation of H-20/H-23 observed in its NOESY spectrum, the 23*S* and 24*S* configurations of compound **3** were established.[15,16] Therefore, the structure of compound **3** was assigned as shown, and the compound was given the trivial name alismanol C.

The physical data of compound **4** resembled those of 16-oxo-11-anhydroalisol A (**14**), a protostane-type triterpenoid,[7b] except for the carbon signal of one extra carbonyl group (δ_C 216.4), which was located at C-7 by the HMBC correlations of C-7 (δ_C 216.4)/H-5 (δ_H 2.81), H-6a (δ_H 2.63). The coupling constant of the doublet of H-24 (J = 1.5 Hz) established the *erythro* 23,24-diol moiety. The ^1H and ^{13}C NMR data and the correlations of H-20/H-23 and H-23/H-24 observed in the NOESY experiment indicated that compound **4** and 16-oxo-11-anhydroalisol A (**14**) had identical absolute configurations of their side chains.[7b] Consequently, the structure of compound **4** was established as 3-oxo-16-oxo-11-anhydroalisol A.

The molecular formula of compound **5** was established as $C_{30}H_{46}O_6$ by HRESIMS. The absorption of an α,β-unsaturated carbonyl group at λ 245.7 nm was observed in the UV spectrum. Comparison of the physical data of **5** with alisol C showed that **5** was an oxidative derivative of alisol C.[18] The oxygenated C-20 could be deduced by the HMBC correlation of H-21 (δ_H 1.51)/C-20 (δ_C 83.3). The doublet of H-24 (d, J = 3.0 Hz) and NOE correlations of H-21/H-23 and H-23/H-24 suggested a C-17 configuration of **5** that is identical to that of alisol C. The 11-OH was determined to be β-oriented by the NOE enhancement of H-11/H-18 observed in the NOESY spectrum. Thus, the structure of compound **5** was defined as 20-hydroxyalisol C.

Compared with alisol A,[17] the resonances of an ethyl group [δ_H 3.53 (2H, m), 1.20 (3H, t, J = 7.0 Hz)] were observed in the NMR spectra of **6**. In the HMBC spectrum of **6**, the correlation of δ_H 3.53/C-25 (δ_C 79.6) confirmed that the ethyl group was attached to 25-OH. Therefore, the structure of compound **6** was elucidated as 25-*O*-ethylalisol A. Compound **6** may be an artifact of alisol A, considering that EtOH was used in the extraction process.

Compound **7** was a white powder with the molecular formula $C_{30}H_{48}NaO_3$, as established by the HRESIMS (m/z 479.3508, calculated for $[M + Na]^+$ 479.3496) and ^{13}C NMR data. Two oxygenated methines were deduced by the proton signals at δ_H 3.38 (m) and 3.80 (d, J = 6.5 Hz) in the ^1H NMR spectrum of **7**. Additionally, the presence of one terminal olefinic bond was confirmed by ^1H and ^{13}C NMR data [δ_H 4.99 (br s), 4.95 (m); δ_C 144.7, 113.9]. On the basis of spectroscopic data, the structure of compound **7** was proposed to be 11-deoxy-25-anhydroalisol E, which was confirmed by the correlations of H-27 (δ_H 1.68)/C-26 (δ_C 113.9), H-24 (δ_H 3.80)/C-26 (δ_C 113.9), H-26a (δ_H 4.99)/C-25 (δ_C 144.7), and H-24 (δ_H 3.80)/C-23 (δ_C 70.8) observed in the HMBC spectrum. The doublet of H-24 (J = 6.5 Hz) in the ^1H NMR spectrum suggested the *threo* 23,24-diol configuration. The (23*S*, 24*R*) absolute configurations were established by the negative Cotton effect at 313 nm in the IECD spectrum using Snatzke's method (Figure 2), similar to alisol E. Accordingly, the structure of compound **7** was assigned as 11-deoxy-25-anhydroalisol E.

DOI: 10.1021/acs.jnatprod.5b00321
J. Nat. Prod. XXXX, XXX, XXX−XXX

Table 1. ^{1}H NMR Spectroscopic Data of Compounds 1−12 (500 MHz, δ in ppm, J in Hz)

no.	1[a]	2[a]	3[a,c]	4[a]	5[b]	6[a,c]	7[b]	8[a]	9[b]	10[b]	11[b]	12[b]
1	2.03 m	1.76 m	2.03 m	1.98 m	2.08 m	2.00 m	2.07 m	2.12 m	2.04 m	2.00 br t (12.5)	2.60 m	2.09 m
	2.19 m	2.14 m	2.19 m	2.26 m	2.20 m	2.15 m	1.44 m	2.21 m	1.76 m	1.62 m	2.71 m	1.75 m
2	2.29 m	2.24 m	2.30 m	2.38 m	2.35 m	2.31 m	1.45 m	2.23 m	2.77 dt (15.0,6.0)	2.68 m		2.73 m
	2.92 m	2.88 m	2.92 m	2.99 m	2.68 m	2.84 m	1.37 m	2.78 m	2.35 m	2.28 m		2.32 m
3											6.09 s	
5	2.50 m	2.44 m	2.35 m	2.81 dd (14.5, 2.0)	2.09 m	2.25 m	1.99 m	2.20 m	1.54 m		2.98 d (13.0)	2.35 m
6	1.53 m	1.48 m	1.53 m	2.39 m	1.39 m	1.36 m	1.43 m	1.54 m	1.40 m	1.52 m	1.54 m	1.59 m
	1.64 m	1.59 m	1.64 m	2.63 m	1.53 m	1.55 m	1.30 m	1.43 m	1.29 m	1.37 m	1.72 m	1.44 m
7	1.82 m	1.41 m	1.84 m		2.11 m	1.36 m	2.01 m	1.43 m	1.64 m	1.88 m	1.21 m	1.98 m
	2.18 m	2.00 m	2.03 m		1.84 m	2.12 m	1.25 m	2.41 m	1.41 m	1.34 m	2.01 m	1.41 m
9	2.53 m	2.48 m	2.53 m	2.99 m	1.89 d (11.0)	1.85 d (11.0)	1.67 m	1.76 d (10.5)		2.31 m	1.82 d (10.5)	2.49 m
11	6.86 dd (10.5, 2.0)	6.77 dd (10.0, 3.0)	6.73 dd (10.0, 3.5)	6.92 dd (10.5, 3.5)	4.04 m	3.88 m	2.49 m	3.86 m	5.39 br d (7.0)	5.72 dd (10.5, 2.0)	3.95 m	6.49 dd (10.0, 2.0)
							1.89 m					
12	6.38 dd (10.0, 3.0)	6.31 dd (10.0, 2.0)	6.38 dd (10.0, 2.0)	6.41 d (10.0, 2.0)	2.44 m	1.55 m	1.52 m	2.16 m	5.51 br d (7.0)	6.18 dd (10.0, 3.5)	2.78 m	5.37 dd (10.0, 3.5)
					2.37 m	2.88 m	1.32 m	3.04 m			2.07 m	
15	1.95 d (18.5)	1.92 m	1.97 d (18.5)	2.28 m	1.91 d (19.0)	2.20 m	1.92 m	6.21 d (5.5)	2.21 m	2.37 m	2.33 m	2.50 d (18.5)
	2.44 d (18.5)	2.44 m	2.48 d (19.0)	2.99 m	2.44 d (19.0)	2.30 m	1.30 m		2.11 m	1.28 m	2.19 m	2.07 d (18.5)
16						2.01 m	2.12 m	6.30 d (5.5)	2.02 m	5.35 dd (10.0, 3.5)	1.39 m	
						2.27 m	2.10 m		1.77 m		1.93 m	
17									1.60 m			
18	1.04 s	1.02 s	1.08 s	1.17 s	0.91 s	1.12 s	1.01 s	0.82 s	0.88 s	0.85 s	0.92 s	1.05 s
19	1.02 s	0.97 s	1.02 s	1.21 s	1.11 s	1.12 s	0.82 s	1.09 s	1.20 s	0.91 s	1.17 s	0.98 s
20	3.26 m	2.99 m	2.86 m	3.03 m		2.90 m	2.83 m	2.90 m	1.44 m	3.14 t (11.0)	2.18 m	
21	1.19 d (7.0)	1.17 s	1.19 d (7.0)	1.25 d (7.0)	1.51 s	1.08 d (7.0)	1.01 d (6.5)	1.13 d (7.0)	0.91 d (6.5)	1.17 d (7.0)	1.02 d (7.0)	2.50 s
22	2.93 m	1.39 m	2.02 m	1.83 m	2.16 m	1.51 m	1.45 m	1.76 m	1.52 m	2.86 m	1.44 m	
	3.29 m	1.96 m	2.37 m	1.98 m	2.44 m	1.64 m	1.37 m	1.53 m	1.27 m	1.29 m	1.68 m	
23		3.23 m	4.83 m	3.66 m	4.34 m	3.79 m	3.38 m	3.63 m	1.40 m		3.79 dd (9.0, 3.0)	
									1.13 m			
24	3.85 s	3.71 d (7.0)	3.45 d (7.0)	3.05 d (1.5)	3.78 d (3.5)	3.13 d (1.5)	3.80 d (6.5)	2.95 d (2.0)	3.35 dd (6.5, 5.5)	3.57 s	3.03 br s	
26	1.25 s	4.86 m	1.18 s	1.16 s	1.27 s	1.27 s	4.99 br s	1.13 s	1.22 s	1.21 s	1.23 s	
		4.92 m					4.95 m					
27	1.13 s	1.61 s	1.21 s	1.17 s	1.28 s	1.26 s	1.68 s	1.14 s	1.17 s	1.21 s	1.28 s	
28	1.16 s	1.11 s	1.16 s	1.19 s	1.08s	1.14 s	1.07 s	1.07 s	1.09 s	1.08 s	1.94 s	1.10 s
29	1.11 s	1.06 s	1.11 s	1.16 s	1.07 s	1.11 s	1.04 s	1.06 s	1.13 s	1.05 s		1.07 s
30	1.17 s	1.17 s	1.19 s	1.23 s	1.34 s	1.24 s	1.10 s	1.10 s	0.60 s	1.08 s	1.16 s	1.22 s

[a]In methanol-d_4. [b]In $CDCl_3$. [c]For the signals of substituents, see the Experimental Section.

A comparison of the ^{1}H NMR data of compound **8** and alisol A showed that **8** displayed one more cyclic olefinic bond [δ_H 6.21 (d, J = 5.5 Hz), δ_H 6.30 (d, J = 5.5 Hz)]. Based on the HMBC correlations between H-15 (δ_H 6.21) and C-14 (δ_C 63.3), C-16 (δ_C 130.7), C-17 (δ_C 139.5), and C-13 (δ_C 146.2) and between H-16 (δ_H 6.30) and C-14 (δ_C 63.3), C-17 (δ_C 139.5), and C-13 (δ_C 146.2), the C-15/C-16 location of the olefinic bond was established. The *erythro* 23,24-diol moiety was established by the proton signal of H-24 [δ_H 2.95 (d, J = 2.0 Hz)], and the α-orientation of H-11 was determined by the correlation of H-11/H-18 in the NOESY experiment. Thus, compared with alisol A, the structure of compound **8** was defined as 15,16-dihydroalisol A.

Protostane triterpenoid (**9**) had the molecular formula $C_{30}H_{48}O_3$ based on HRESIMS and ^{13}C NMR data. Two cyclic olefinic proton signals were observed at δ_H 5.51 (d, J = 7.0 Hz) and 5.39 (d, J = 7.0 Hz) in the ^{1}H NMR spectrum. Combined with the ^{13}C NMR data (δ_C 144.6, 142.9, 119.9, 117.3), two olefinic bonds were deduced in the structure of **9**. The positions of the double bonds were established as C-9/C-11 and C-12/C-13 by the correlations of H-11 (δ_H 5.39)/C-12 (δ_C 119.9), C-13 (δ_C 142.9), H-12 (δ_H 5.51)/C-14, and H-19 (1.20)/C-9 (δ_C 144.6) in the HMBC spectrum. Additionally, two hydroxy groups were assigned at C-24 and C-25 based on the HMBC correlations between H-24 (δ_H 3.35) and C-22, C-23 and between C-25 (δ_C 73.2) and H-24, H-26, H-27. The IECD spectra based on Snatzke's method showed a positive Cotton effect at 304 nm (Figure 2), which established the 24*S* configuration of **9**. Therefore, the structure of compound **9** was elucidated as shown in Figure 1 and named alismanol D.

HRESIMS and 1D NMR data revealed that **10** was also a protostane triterpenoid with a C-3 carbonyl group, C-11/C-12 and C-13/C-17 cyclic double bonds, and oxygenated carbons (C-16, C-24, C-25). This suggested that the structure of **10** was similar to 24-de-*O*-acetylalisol O,[18] except for C-23 and C-24. The C-23 carbonyl group was established by HMBC

DOI: 10.1021/acs.jnatprod.5b00321
J. Nat. Prod. XXXX, XXX, XXX−XXX

Table 2. ^{13}C NMR Spectroscopic Data of Compounds 1−12 (125 MHz, $CDCl_3$)

no.	1[a]	2[a]	3[a,c]	4[a]	5[b]	6[a,c]	7[b]	8[a]	9[b]	10[b]	11[b]	12[b]
1	32.3	33.3	32.3	33.5	30.7	32.0	31.8	32.0	36.7	32.1	42.3	32.3
2	34.3	34.4	34.4	34.3	33.5	34.7	33.8	34.7	34.9	33.5	202.5	33.2
3	222.3	222.3	222.3	220.4	219.3	223.4	220.2	223.4	216.8	219.5	131.4	218.6
4	47.3	48.7	47.3	48.0	47.2	48.1	47.0	48.2	47.5	47.2	162.7	47.2
5	48.5	47.3	48.4	44.7	48.2	49.7	48.3	49.5	50.8	46.4	45.6	46.0
6	20.3	20.3	20.3	39.0	20.1	20.5	20.1	21.1	28.4	19.2	22.4	19.2
7	33.3	32.2	33.3	216.4	34.8	35.4	34.1	36.5	31.5	31.0	34.7	31.2
8	40.6	40.5	40.5	47.4	40.2	42.0	40.6	40.4	50.4	39.8	40.7	48.9
9	49.1	49.2	49.1	48.0	48.7	50.7	44.0	50.1	144.6	47.1	50.9	48.4
10	37.2	37.2	37.2	36.9	36.8	38.2	36.3	38.1	37.2	36.0	28.5	36.1
11	123.3	123.3	123.0	123.6	70.0	70.5	23.2	71.4	117.3	131.6	70.9	145.5
12	140.1	140.1	140.6	136.8	36.3	35.1	22.6	35.3	119.9	120.9	34.5	124.3
13	173.1	174.3	174.0	171.6	174.7	139.0	140.1	146.2	142.9	145.4	136.3	182.3
14	49.6	49.6	49.7	53.2	50.0	58.3	57.4	63.3	50.4	53.9	57.2	41.1
15	45.4	45.6	45.4	48.7	45.6	31.7	31.1	143.4	37.9	38.6	29.7	44.8
16	210.2	210.5	210.5	211.2	206.3	30.3	28.9	130.7	28.0	82.9	30.8	204.2
17	140.0	139.7	139.5	141.1	141.9	136.8	134.2	139.5	51.1	133.9	137.1	131.6
18	22.2	22.3	22.5	17.2	23.1	23.7	22.9	22.9	25.4	22.6	23.9	22.0
19	24.9	24.9	24.9	25.0	25.5	26.0	23.6	25.7	23.7	24.6	28.4	24.8
20	26.3	27.7	27.6	27.7	83.3	29.8	28.4	28.8	36.1	47.4	29.4	197.1
21	19.4	20.0	20.4	19.8	26.3	21.1	20.4	21.8	18.4	20.6	20.2	30.9
22	46.7	39.0	34.3	41.2	46.9	41.8	38.4	43.1	33.1	28.8	40.1	
23	213.7	72.2	72.9	70.1	72.6	69.7	70.8	70.3	23.3	216.4	69.6	
24	83.7	81.3	79.5	79.4	91.3	79.5	79.5	79.5	78.7	83.1	77.4	
25	73.2	146.5	75.0	74.5	71.1	79.6	144.7	74.6	73.2	72.6	74.3	
26	27.3	113.9	26.0	27.1	25.5	23.4	113.9	27.0	26.6	26.5	26.1	
27	25.1	18.1	27.0	26.4	26.8	21.6	17.9	26.6	22.1	25.4	27.4	
28	29.5	29.5	29.5	29.0	29.6	29.9	29.3	29.8	25.5	29.3	25.1	29.2
29	19.7	19.7	19.7	19.9	19.9	20.8	19.7	20.5	22.5	19.4		19.4
30	23.9	24.5	24.4	17.2	23.2	24.5	23.6	18.0	15.8	23.6	23.4	23.9

[a]In methanol-d_4. [b]In $CDCl_3$. [c]For the signals of substituents, see the Experimental Section.

correlations between C-23 (δ_C 216.4) and H-21, H-22, H-24. A 16,24-oxepane ring was also established by the correlation of H-24 (δ_H 3.57)/C-16 (δ_C 82.9), similar to that in alismaketone B 23-acetate (**18**).[2b] Thus, the 2D structure of **10** was established. In a NOESY experiment, H-16 exhibited correlations with H-18 and H-21, which indicated the α orientation of H-16. The NOE correlations of H-24/H-22a and H-22a/H-21 also established a 24*R* configuration. Therefore, the structure of compound **10** was defined as shown and named alismanol E.

Compound **11** was obtained as a white powder. Analyses of HRESIMS and ^{13}C NMR data suggested a molecular formula of $C_{29}H_{46}O_5$. The UV spectrum displayed the absorption of an α,β-unsaturated carbonyl moiety at 240.7 nm. The presence of seven methyl groups [δ_H 1.94, 1.28, 1.23, 1.17, 1.16, 0.92 (each 3H, s) and δ_H 1.02 (3H, d, J = 7.0 Hz)] was deduced from the ^1H NMR spectrum. Twenty-nine carbon signals were observed in the ^{13}C NMR spectrum. Analyses of the physical data indicated that compound **11** possessed a 29-norprotostane skeleton. Compared with alisol A, **11** possessed identical structures of rings B and C, as well as the C-17 side chain, which were confirmed by the HMBC and $^1H-^1H$ COSY spectra. For the structure of ring A, the HMBC correlations of H-1a (δ_H 2.71)/C-3 (δ_C 202.5); H-3 (δ_H 6.09)/C-28 (δ_C 25.1), C-5 (δ_C 45.6); and H-28 (δ_H 1.91)/C-5 (δ_C 45.6), C-3 (δ_C 131.4), C-4 (δ_C 162.7) implied the presence of the α,β-unsaturated carbonyl and 28-CH_3 groups, as well as the absence of 29-CH_3. The NOESY spectrum displayed the correlation of H-11/H-18, which suggested that 11-OH was β oriented. The singlet of H-24 in the ^1H NMR spectrum also indicated the *erythro* 23,24-diol moiety, which was classified as an alisol A series with a 23*S*, 24*R* absolute configuration. Therefore, the structure of compound **11** was determined to be a 29-nortriterpenoid as shown and named alismanol F.

Alismanol G (**12**) was determined to have a molecular formula of $C_{24}H_{32}O_3$ from the HRESIMS and ^{13}C NMR data. A conjugated dienone moiety was deduced from the UV absorption maximum at λ_{max} 291.2 nm. The proton signals of six methyl groups [δ_H 2.50, 1.22, 1.10, 1.07, 1.05, 0.98 (each 3H, s)] and two olefinic protons at δ_H 6.49 (d, J = 10.0, 2.0 Hz) and 5.37 (d, J = 10.0, 3.5 Hz) were observed from the ^1H NMR spectrum. Twenty-four carbons were displayed in the ^{13}C NMR spectrum, including the signals of a conjugated dienone moiety and two carbonyl groups. On the basis of the physical data, a 24-nor pentacyclic triterpenoid structure was deduced for **12**, which was similar to the protostane skeleton, except for the absence of the C-17 side chain. Further analysis of the ^1H and ^{13}C NMR data suggested that **12** had the same pentacyclic structure as compound **1**. An acetyl moiety [δ_H 2.50 (3H, s), δ_C 197.1, 37.9] was assigned at C-17 by the HMBC correlations of δ_H 2.50/C-16 (δ_C 204.2), C-17 (δ_C 131.6), and C-20 (δ_C 197.1). Accordingly, compound **12** was determined to be the 24-norprotostane triterpenoid as shown and named alismanol G.

The nine known compounds were identified as alisol E 24-acetate (**13**),[19] 16-oxo-11-anhydroalisol A (**14**),[7b] alisol A (**15**),[4b] 11-deoxyalisol A (**16**),[15] alisol B 23-acetate (**17**),[20]

DOI: 10.1021/acs.jnatprod.5b00321
J. Nat. Prod. XXXX, XXX, XXX−XXX

alismaketone B 23-acetate (**18**),[2b] 24-deacetylalisol O (**19**),[18] alisol O (**20**),[18] 25-anhydroalisol F (**21**),[4d] and alisol P (**22**)[21] from their physical data upon comparison with values reported in the literature.

The hCE-2 inhibitory effects of compounds **1**−**22** were evaluated in a bioassay. As shown in Table 3, most of the isolated protostanes exhibited inhibitory effects toward hCE-2. Compounds **2**, **6**, **9**, and **11** showed moderate inhibitory effects, with IC_{50} values of <10 μM, while the IC_{50} value of BNNP (bis-*para*-nitrophenylphosphate, a reported potent hCE inhibitor) against hCE-2 was 4.03 μM.[22,23] None of the isolated compounds exhibited inhibitory effects against hCE-1.

Table 3. Human Carboxylesterase 2 (hCE-2) Inhibitory Effects of Compounds 1−22

compound	IC_{50} (μM)	compound	IC_{50} (μM)
1	10.14	**12**	71.59
2	8.68	**13**	10.79
3	33.41	**14**	22.74
4	100	**15**	100
5	100	**16**	4.63
6	4.72	**17**	36.18
7	17.44	**18**	41.14
8	25.7	**19**	17.27
9	4.58	**20**	24.33
10	58.79	**21**	10.87
11	2.02	**22**	20.85

Owing to the potential inhibition of hCE-2 by compound **11**, the inhibition kinetics and K_i value were further investigated (Figure 3). The Dixon and Lineweaver−Burk plots were evaluated to determine the inhibition type, and a second plot that was created using the slopes obtained from the Lineweaver−Burk plot and the concentrations of compound **11** was used to calculate the K_i value. The results showed that compound **11** inhibited hCE-2 with a fixed inhibition model. The K_i value was calculated as 1.7 μM for the activity of hCE-2.

The interaction mechanism between compound **11** and hCE-2 was also investigated. Compound **11** was chosen for docking into hCE-2 with the Flex-X package to generate 20 possible binding orientations. As shown in Figure 4A, compound **11** could be well docked into the catalytic site of hCE-2. The side chain of **11** was only 2.1 Å from the catalytic amino acid Ser-200 in hCE-2 (Figure 4B). The docking scores were expressed in $-\log(K_d)$ units, and the docking results indicated that compound **11** exhibited high hCE-2 binding affinities ($-\log(K_d)$ = 9.8).[24] Moreover, hydrogen bonds with Ser-200, Glu-225, and Arg-438 and van der Waals interactions could also be observed in the docking results (Figure 4B), which was consistent with the experimental data.

Protostane triterpenoids are stereoisomers of dammarane triterpenoids that possess a tetracyclic skeleton with characteristic orientations of 8α-CH_3, 9β-H, 10β-CH_3, 13α-H, and 14β-CH_3.[4] Protostane triterpenoids mainly differ in their prevalent oxygenation patterns. *Alisma* protostane triterpenoids can be conveniently classified into the alisol A, B, and E series on the basis of differences in their side chains, such as the configurations of C-23 and C-24.[15] The alisol A series protostane triterpenoids possess oxygenation at C-23, C-24, and C-25 and 20*R*, 23*S*, and 24*R* configurations in their side chains. However, they do not possess 24,25-epoxy groups. The alisol B series triterpenoids possess a 24,25-epoxy group with a 20*R*, 23*S*, 24*R* configuration for the side chain. The alisol E series protostane triterpenoids have a similar side chain to alisol A except for the 24*S* configuration. These characteristics of *Alisma* protostane triterpenoids were helpful in elucidating the structures of the isolated compounds. On the basis of physical data and literature analyses, the structures of isolated compounds **1**−**22** were elucidated and classified into the alisol A (**4**, **6**, **8**, **10**, **14**−**16**, **18**−**21**), alisol B (**5**, **17**), and alisol E

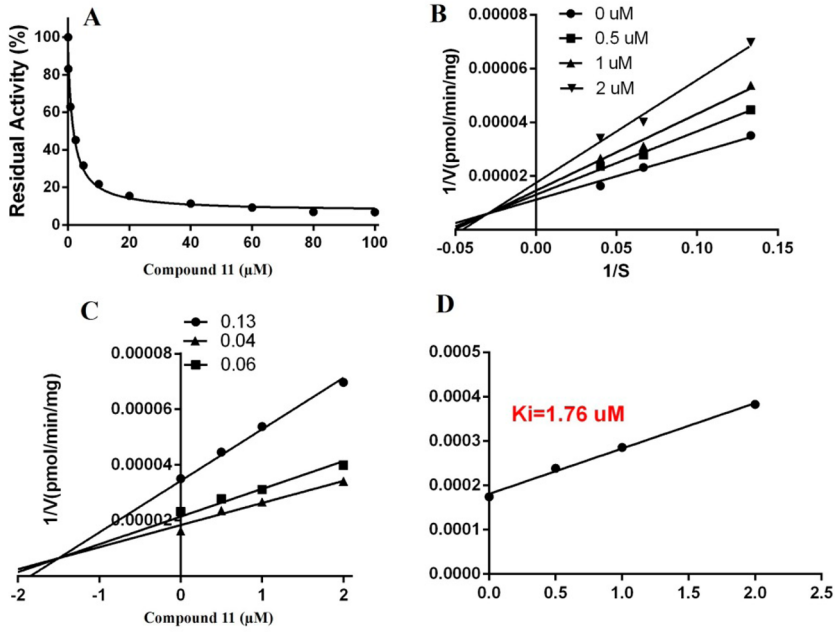

Figure 3. Evaluation of the inhibition of recombinant hCE-2 by compound **11**. (A) Compound **11** exhibited concentration-dependent inhibition of hCE-2. (B) Dixon plot of hCE-2 inhibition by compound **11**. (C) Lineweaver−Burk plot of inhibition of hCE-2 by compound **11**. (D) Second inhibition plot of recombinant hCE-2 by compound **11**. The data points represent the means of duplicate experiments.

DOI: 10.1021/acs.jnatprod.5b00321
J. Nat. Prod. XXXX, XXX, XXX−XXX

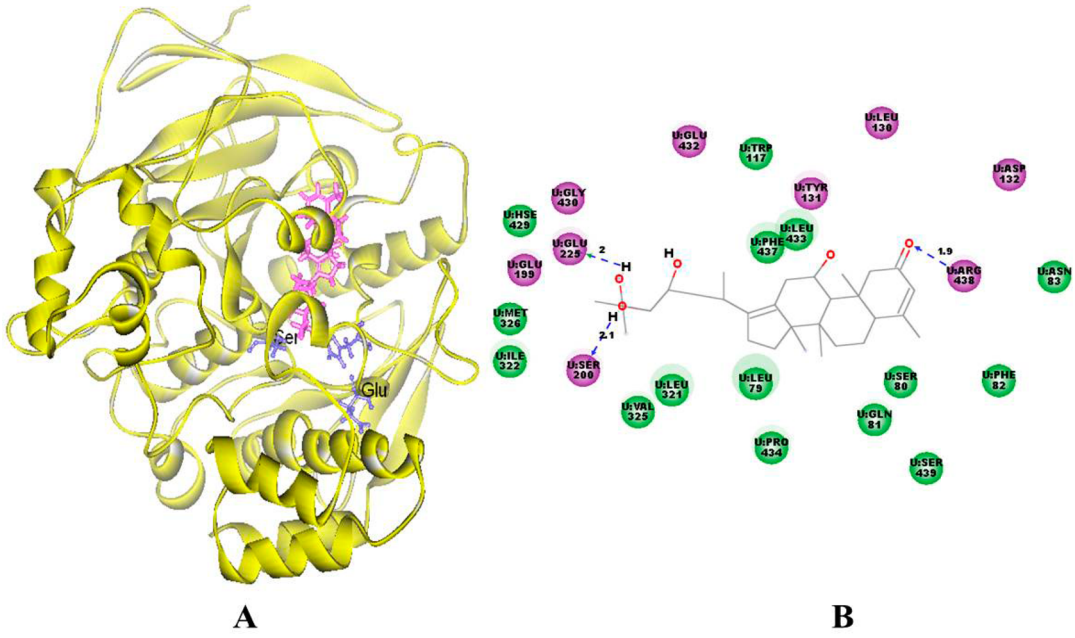

Figure 4. (A) Possible binding modes of the amino acid residues Ser-221, Glu-343, and His-467 in an active site triad of hCE-2 with compound **11**. The modeled hCE-2 is yellow, compound **11** is magenta, and the active site amino acids are shown in blue. A detailed view of the binding site shows that the Ser-228 residue is close to the side chain of compound **11**. (B) Schematic representation of the proposed binding modes of the active compound **11** (gray) in the active site of the modeled hCE-2. Residues involved in hydrogen bonds, charge interactions, or polar interactions are represented by magenta-colored circles; residues involved in van der Waals interactions are represented by green circles. The solvent-accessible surface of an interacting residue is represented by a halo around the residue. The diameter of the circle is proportional to the solvent-accessible surface. Hydrogen bond interactions with amino acid side chains are represented by a blue dashed line with an arrowhead directed toward the electron donor, and their average distances are denoted by numbers beside the dashed lines.

series (**1**−**3**, **7**, **13**), 2,3-*seco* protostane (**22**), and nor-triterpenoids (**11**, **12**).

On the basis of the structures and hCE-2 inhibitory effects analyses, a preliminary structure−activity relationship (SAR) is evident. The hydroxy groups located at C-23, C-24, or C-25 were key factors for the hydrogen bonds between triterpenoids and the hCE-2 enzyme. Therefore, the oxygenated moieties enhanced the inhibitory effects. However, the alisol A and E series protostane triterpenoids displayed greater potential inhibitory effects than the alisol B series, which suggested that the 24,25-epoxy group had a negative effect. Compound **12** exhibited a poor inhibitory effect, which may be ascribed to the absence of an oxygenated side chain. The nor-triterpenoids **11** and **22** also displayed moderate inhibitory effects, which indicated that ring A was not a key moiety for the activity.

EXPERIMENTAL SECTION

General Experimental Procedures. Optical rotations were recorded on a JASCO P2000 automatic digital polarimeter. UV spectra were measured on a JASCO V-650 spectrophotometer. ECD spectra were measured on a JASCO J-815 spectropolarimeter. NMR spectra were measured with a Bruker-500 spectrometer in $CDCl_3$ and methanol-d_4 with TMS as the internal standard. ESIMS data were obtained on an API 3200 mass spectrometer (AB SCIEX, Framingham, MA, USA). HRESIMS spectra were collected on an Agilent 1100 series LC/MSD ion trap mass spectrometer. Analytical HPLC was conducted on an UltiMate 3000 instrument (Thermo Scientific Dionex) equipped with a diode array detector (DAD). Preparative HPLC was performed on an Agela instrument with a UV detector and a YMC C_{18} column (250 × 20 mm, 5 μm). Column chromatography was performed with silica gel (160−200 mesh, Qingdao Marine Chemical Inc., Qingdao, People's Republic of China). TLC was performed on glass precoated silica gel GF254 plates. Spots were visualized under UV light or by spraying with 10% sulfuric acid in EtOH followed by heating at 110 °C.

Plant Material. Dried rhizomes of *A. orientale* (301114120P) were purchased in January 2013 from Beijing Tongrentang Co., Ltd., People's Republic of China.

Extraction and Isolation. Dried rhizomes of *A. orientale* (4 kg) were powdered and extracted with 80% EtOH (10 L × 3) under reflux. The EtOH was evaporated *in vacuo*, and the aqueous residue was diluted with H_2O and partitioned successively with petroleum ether, $CHCl_3$, and *n*-BuOH. The $CHCl_3$ extract (240 g) was passed through a silica gel column by eluting with $CHCl_3$−MeOH (100:1−4:1) in sequence to give fractions 1−24. Fr.5 (7.4 g) was subjected to column chromatography through RP18 with MeOH−H_2O (30−80%) and purified by preparative HPLC (detected at 210, 250, and 290 nm, respectively, at 8 mL/min, 40−60% CH_3CN−H_2O) to give compounds **1** (2.3 mg), **2** (3.5 mg), **5** (5.2 mg), **7** (7.1 mg), **14** (6.3 mg), **15** (7.7 mg), **16** (5.4 mg), and **19** (3.2 mg). Fr.6 was subjected to an RP-18 column with CH_3CN−water (20−60%) and subsequently purified by pre-HPLC to yield compounds **3** (4.4 mg), **4** (4.8 mg), **6** (3.6 mg), **8** (5.5 mg), **9** (3.0 mg), **11** (5.3 mg), **12** (3.1 mg), and **13** (3.5 mg). Fr.7 was subjected to an RP 18 column eluted with MeOH−H_2O (20−80%) to yield 20 fractions, which were purified with pre-HPLC to yield compounds **10** (2.8 mg), **14** (3.6 mg), **17** (9.0 mg), **18** (8.3 mg), **20** (4.7 mg), **21** (4.2 mg), and **22** (5.7 mg).

*Alismanol A (**1**):* white, amorphous powder; $[\alpha]_D^{25}$ −40 (*c* 0.1, CH_3OH); UV (MeOH) λ_{max} (log ε) 289.0 (4.07) nm; $Mo_2(OAc)_4$-induced ECD (DMSO) 305.5 ($\Delta\varepsilon$ +0.15) nm; ^{1}H NMR (methanol-d_4, 500 MHz), see Table 1; ^{13}C NMR (methanol-d_4, 125 MHz), see Table 2; HRESIMS *m*/*z* 507.3085 $[M + Na]^+$ (calculated for $C_{30}H_{44}NaO_5$, 507.3081).

*Alismanol B (**2**):* white, amorphous powder; $[\alpha]_D^{25}$ −36 (*c* 0.1, CH_3OH); UV (MeOH) λ_{max} (log ε) 290.0 (4.08) nm; $Mo_2(OAc)_4$-induced ECD (DMSO) 310 ($\Delta\varepsilon$ −0.8) nm; ^{1}H NMR (methanol-d_4, 500 MHz), see Table 1; ^{13}C NMR (methanol-d_4, 125 MHz), see Table 2; HRESIMS *m*/*z* 491.3138 (calculated for $C_{30}H_{44}NaO_4$, 4491.3132).

DOI: 10.1021/acs.jnatprod.5b00321
J. Nat. Prod. XXXX, XXX, XXX−XXX

*Alismanol C (**3**):* white, amorphous powder; $[\alpha]_D^{25}$ −59 (*c* 0.1, CH_3OH); UV (MeOH) λ_{max} (log ε) 290.0 (4.17) nm; ^1H NMR (methanol-d_4, 500 MHz), see Table 1 and δ_H 2.06 (3H, s, Ac); ^{13}C NMR (methanol-d_4, 125 MHz), see Table 2 and δ_C 21.4 (Ac), 172.5 (Ac); HRESIMS *m*/*z* 551.3352 (calculated for $C_{32}H_{48}NaO_6$, 551.3343).

*3-Oxo-16-oxo-11-anhydroalisol A (**4**):* white, amorphous powder; $[\alpha]_D^{25}$ −40 (*c* 0.1, CH_3OH); UV (MeOH) λ_{max} (log ε) 290.3 (4.02); ^1H NMR (methanol-d_4, 500 MHz), see Table 1; ^{13}C NMR (methanol-d_4, 125 MHz), see Table 2; HRESIMS *m*/*z* 501.3211 (calculated for $C_{30}H_{45}O_6$, 501.3211).

*20-Hydroxyalisol C (**5**):* white, amorphous powder; $[\alpha]_D^{25}$ −47 (*c* 0.1, CH_3OH); UV (MeOH) λ_{max} (log ε) 245.7 (3.55) nm; ^1H NMR ($CDCl_3$, 500 MHz), see Table 1; ^{13}C NMR ($CDCl_3$, 125 MHz), see Table 2; HRESIMS *m*/*z* 525.3186 $[M + Na]^+$ (calculated for $C_{30}H_{46}NaO_6$, 525.3187).

*25-O-Ethylalisol A (**6**):* white, amorphous powder; $[\alpha]_D^{25}$ −25 (*c* 0.1, CH_3OH); UV (MeOH) λ_{max} (log ε) 280.4 (3.99) nm; $Mo_2(OAc)_4$-induced ECD (DMSO) 313 ($\Delta\varepsilon$ −0.64) nm; ^1H NMR (methanol-d_4, 500 MHz), see Table 1 and δ_H 3.53 (2H, m, Et), 1.20 (3H, t, *J* = 7.0 Hz, Et); ^{13}C NMR (methanol-d_4, 125 MHz), see Table 2 and δ_C 57.9 (Et), 16.5 (Et); HRESIMS *m*/*z* 541.3871 (calculated for $C_{32}H_{54}NaO_5$, 541.3863).

*11-Deoxy-25-anhydroalisol E (**7**):* white, amorphous powder; $[\alpha]_D^{25}$ +28 (*c* 0.1, CH_3OH); UV (MeOH) λ_{max} (log ε) 210.1 (4.21) nm; $Mo_2(OAc)_4$-induced ECD (DMSO) 313.5 ($\Delta\varepsilon$ −0.81) nm; ^1H NMR ($CDCl_3$, 500 MHz), see Table 1; ^{13}C NMR ($CDCl_3$, 125 MHz), see Table 2; HRESIMS *m*/*z* 479.3508 (calculated for $C_{30}H_{48}NaO_3$, 479.3496).

*15,16-Dihydroalisol A (**8**):* white, amorphous powder; $[\alpha]_D^{25}$ −35 (*c* 0.1, CH_3OH); UV (MeOH) λ_{max} (log ε) 285.3 (4.13) nm; ^1H NMR (methanol-d_4, 500 MHz), see Table 1; ^{13}C NMR (methanol-d_4, 125 MHz), see Table 2; HRESIMS *m*/*z* 511.3408 (calculated for $C_{30}H_{48}NaO_6$, 511.3394).

*Alismanol D (**9**):* white, amorphous powder; $[\alpha]_D^{25}$ +52 (*c* 0.1, CH_3OH); UV (MeOH) λ_{max} (log ε) 280.5 (3.85) nm; $Mo_2(OAc)_4$-induced ECD (DMSO) 304 ($\Delta\varepsilon$ +1.09) nm; ^1H NMR ($CDCl_3$, 500 MHz), see Table 1; ^{13}C NMR ($CDCl_3$, 125 MHz), see Table 2; HRESIMS *m*/*z* 479.3505 (calculated for $C_{30}H_{48}NaO_3$, 479.3496).

*Alismanol E (**10**):* white, amorphous powder; $[\alpha]_D^{25}$ +44 (*c* 0.1, CH_3OH); UV (MeOH) λ_{max} (log ε) 290.0 (3.77) nm; ^1H NMR ($CDCl_3$, 500 MHz), see Table 1; ^{13}C NMR ($CDCl_3$, 125 MHz), see Table 2; HRESIMS *m*/*z* 491.3140 (calculated for $C_{30}H_{44}NaO_4$, 491.3132).

*Alismanol F (**11**):* white, amorphous powder; $[\alpha]_D^{25}$ +48 (*c* 0.1, CH_3OH); UV (MeOH) λ_{max} (log ε) 240.7 (3.37) nm; ^1H NMR ($CDCl_3$, 500 MHz), see Table 1; ^{13}C NMR ($CDCl_3$, 125 MHz), see Table 2; HRESIMS *m*/*z* 473.2578 (calculated for $C_{30}H_{46}NaO_6$, 473.2539).

*Alismanol G (**12**):* white, amorphous powder; $[\alpha]_D^{25}$ +27 (*c* 0.1, CH_3OH); UV (MeOH) λ_{max} (log ε) 293.1 (4.10) nm; ^1H NMR ($CDCl_3$, 500 MHz), see Table 1; ^{13}C NMR ($CDCl_3$, 125 MHz), see Table 2; HRESIMS *m*/*z* 391.2245 (calculated for $C_{24}H_{32}NaO_3$, 391.2244).

Inhibitory Effects on hCE-1 and hCE-2. Compounds **1**−**22** were dissolved in MeOH and diluted to final concentrations of 0.1, 1.0, 5.0, 10.0, 20.0, 50.0, 100.0, and 200.0 μM. The hydrolysis of triterpenoids **1**−**22** by hCE-1 and hCE-2 was carried out at 37 °C in a 96-well plate format with the probe substrates 2-(2′-benzoyl-3′-methoxylphenyl)-benzothiazole (BMBT) and 4-benzoyl-*N*-butyl-1,8-naphthalimide (MPN), respectively. The detected fluorescence signals of hCE-1 and hCE-2 were at 488 and 564 nm, respectively. The probe substrate groups (without evaluated compounds) were used as control. Other procedures, including the termination step, were performed as previously described.[25]

Molecular Modeling. Structural modeling[12d] of hCE-2 was used to provide insights into hCE-2-mediated compound **11** hydrolysis. The 2D structure of the drug molecule used in this study was generated using ChemDraw with standard bond lengths and angles (shown in Figure 4B). The Tripos force field was employed to minimize the molecular energy and to search for the most stable conformation using the Powell conjugate gradient algorithm and a convergence criterion of 0.001 kcal/mol. The energy gradient limit was set at 0.05 kcal/mol·Å. The compound's partial charges were calculated using the Gasteiger−Huckel method and the SYBYL-X program (Tripos Inc.).

The docking of ligand into the catalytic domain of the hCE-2 model was performed using Surflex-Dock (within Sybyl-X1.2, Tripos International). The protocol was generated using an automated method, a threshold of 0.50, and a bloat value of 2. The Surflex-Dock mode was used, and all of the other parameters were set to the default values. The Total-Score function was used to rank the docked compound poses, and the top 20 ranked poses for each compound were examined visually.

■ ASSOCIATED CONTENT

Supporting Information

The Supporting Information is available free of charge on the ACS Publications website at DOI: 10.1021/acs.jnatprod.5b00321.

Copies of spectra of compounds **1**−**12** (PDF)

■ AUTHOR INFORMATION

Corresponding Authors

*E-mail (C. Wang): wach_edu@dlmedu.edu.cn.

*Tel (X. C. Ma): +86-411-86110419. Fax: +86-411-86110408. E-mail: maxc1978@163.com.

Notes

The authors declare no competing financial interest.

■ ACKNOWLEDGMENTS

This work was supported by the National Natural Science Foundation of China (Nos. 81274047, 81473334, 81503201, and 81303146), Education Department and Distinguished professor of Liaoning Province (LR2014025, L2014352), Outstanding Youth Science and Technology Talents of Dalian (2014J11JH132), and Innovation Team of Dalian Medical University.

■ REFERENCES

(1) Zhang, Z.; Wang, D.; Zhao, Y.; Gao, H.; Hu, Y. H.; Hu, J. F. *Nat. Prod. Res.* **2009**, *23*, 1013−1020.

(2) (a) Yoshikawa, M.; Hatakeyama, S.; Tanaka, N. *Chem. Pharm. Bull.* **1993**, *41*, 1948−1954. (b) Peng, G. P.; Tian, G.; Matsuda, H.; Kageura, T.; Toguchida, I.; Murakami, T.; Kishi, A.; Yoshikawa, M. *Bioorg. Med. Chem. Lett.* **1999**, *9*, 3081−3086. (c) Peng, G. P.; Lou, F. C.; Huang, X. F.; Tian, G. *Tetrahedron* **2002**, *58*, 9045−9048. (d) Huang, X. F.; Lou, F. C. *Phytochemistry* **2003**, *63*, 877−881.

(3) (a) Yoshikawa, M.; Tomohiro, N.; Murakami, T.; Ikebata, A.; Matsuda, H.; Matsuda, H.; Kubo, M. *Chem. Pharm. Bull.* **1999**, *47*, 524−528. (b) Peng, G. P.; Tian, G.; Huang, X. F.; Lou, F. C. *Phytochemistry* **2003**, *63*, 877−881.

(4) (a) Murata, T.; Imai, Y.; Hirata, T.; Miyamoto, M. *Chem. Pharm. Bull.* **1970**, *18*, 1347−1353. (b) Murata, T.; Miyamoto, M. *Chem. Pharm. Bull.* **1970**, *18*, 1354−1361. (c) Yoshiaysu, F.; Geng, P. W.; Wang, R.; Toshihide, Y.; Kazuyuki, N. *Planta Med.* **1988**, *54*, 445−447. (d) Hua, X. Y.; Guo, Y. Q.; Gao, W. Y.; Zhang, T. J.; Che, H. X. *J. Asian Nat. Prod. Res.* **2008**, *10*, 487−490.

(5) Geng, P. W.; Yoshiyasu, F.; Toshihide, Y.; Wang, R.; Bao, J. X.; Kazuyuki, N. *Phytochemistry* **1988**, *27*, 1161−1164.

(6) Li, Q.; Qu, H. *Fitoterapia* **2012**, *83*, 1046−1053.

(7) (a) Matsuda, H.; Kobayashi, G.; Yamahara, J.; Fujimura, H.; Kurahashi, K.; Fujiwara, M. *Life Sci.* **1987**, *41*, 1845. (b) Kato, T.; Tomita, M.; Takigawa, M.; Iwasaki, H.; Hirukawa, T.; Yamahara, J. *Bull. Chem. Soc. Jpn.* **1994**, *67*, 1394−1398.

DOI: 10.1021/acs.jnatprod.5b00321
J. Nat. Prod. XXXX, XXX, XXX−XXX

(8) Zhang, C. F.; Zhou, A. C.; Zhang, M. *Chin. J. Chin. Mater. Med.* **2009**, *34*, 994−998.
(9) Zhang, Q.; Jiang, Z. Y.; Luo, J.; Cheng, P.; Ma, Y. B.; Zhang, X. M.; Zhang, F. X.; Zhou, J.; Chen, J. J. *Bioorg. Med. Chem. Lett.* **2008**, *18*, 4647−4650.
(10) Takai, S.; Matsuda, A.; Usami, Y.; Adachi, T.; Sugiyama, T.; Katagiri, Y.; Tatematsu, M.; Hirano, K. *Biol. Pharm. Bull.* **1997**, *20*, 869−873.
(11) Xu, J. S.; Li, Y. Y.; Chen, W. D.; Xu, Y.; Yin, L. Y.; Ge, X. M.; Jadhav, K.; Adorini, L.; Zhang, Y. Q. *Hepatology* **2014**, *59*, 1761−1771.
(12) (a) Chanteux, H.; Van Bambeke, F.; Mingeot-Leclercq, M. P.; Tulkens, P. M. *Antimicrob. Agents Chemother.* **2005**, *49*, 1279−1288. (b) Imai, T.; Ohura, K. *Curr. Drug Metab.* **2010**, *11*, 793−805. (c) Laizure, S. C.; Herring, V.; Hu, Z. Y.; Witbrodt, K.; Parker, R. B. *Pharmacotherapy* **2013**, *33*, 210−222. (d) Feng, L.; Liu, Z. M.; Xu, L.; Lv, X.; Ning, J.; Hou, J.; Ge, G. B.; Cui, J. N.; Yang, L. *Chem. Commun.* **2014**, *50*, 14519−14522.
(13) Zhao, M.; Godecke, T.; Gunn, J.; Duan, J. A.; Che, C. T. *Molecules* **2013**, *18*, 4054−4080.
(14) (a) Di Bari, L.; Pescitelli, G.; Pratelli, C.; Pini, D.; Salvadori, P. *J. Org. Chem.* **2001**, *66*, 4819−4825. (b) Gorecki, M.; Jabłonska, E.; Kruszewska, A.; Suszczynska, A.; Urbanczyk, L. Z.; Gerards, M.; Morzycki, J. W.; Szczepek, W. J.; Frelek, J. *J. Org. Chem.* **2007**, *72*, 2906−2916. (c) Liu, J.; Liu, Y. B.; Si, Y. K.; Yu, S. S.; Qu, J.; Xu, S. *Steroids* **2009**, *74*, 51−61. (d) Yan, H. J.; Wang, J. S.; Kong, L. Y. *J. Nat. Prod.* **2014**, *77*, 234−242.
(15) Makabel, B.; Zhao, Y. Y.; Wang, B.; Bai, Y. J.; Zhang, Q. Y.; Wu, L.; Lv, Y. *Chem. Pharm. Bull.* **2008**, *56*, 41−45.
(16) Zhang, F.; Wang, J. S.; Gu, Y. C.; Kong, L. Y. *J. Nat. Prod.* **2012**, *75*, 538−546.
(17) Nakajma, Y.; Satoh, Y.; Katsumata, M.; Tsujiyama, K.; Ida, Y.; Shoji, J. *Phytochemistry* **1994**, *36*, 119−127.
(18) Zhou, A. C.; Zhang, C. F.; Zhang, M. *Zhongguo Tianran Yaowu* **2008**, *6*, 109−111.
(19) Peng, G. P.; Zhu, G. Y.; Lou, F. C. *Nat. Prod. Res. Dev.* **2002**, *14*, 7−10.
(20) Yoshikawa, M.; Hatakeyama, S.; Tanaka, N.; Matsuoka, T.; Yamahara, J.; Murakami, N. *Chem. Pharm. Bull.* **1993**, *41*, 2109−2112.
(21) Zhao, M.; Xu, L. J.; Che, C. T. *Phytochemistry* **2008**, *69*, 527−532.
(22) Li, Y. G.; Hou, J.; Li, S. Y.; Lv, X.; Ning, J.; Wang, P.; Liu, Z. M.; Ge, G. B.; Ren, J. Y.; Yang, L. *Fitoterapia* **2015**, *101*, 99−106.
(23) Eng, H.; Niosi, M.; McDonald, T. S.; Wolford, A.; Chen, Y.; Simila, S. T.; Bauman, J. N.; Warmus, J.; Kalgutkar, A. S. *Xenobiotica* **2010**, *40*, 369−380.
(24) Gertsch, J.; Leonti, M.; Raduner, S.; Racz, I.; Chen, J. Z.; Xie, X. Q.; Altmann, K. H.; Karsak, M.; Zimmer, A. *Proc. Natl. Acad. Sci. U. S. A.* **2008**, *105*, 9099−9104.
(25) Liu, Z. M.; Feng, L.; Hou, J.; Lv, X.; Ning, J.; Ge, G. B.; Wang, K. W.; Cui, J. N.; Yang, L. *Sens. Actuators, B* **2014**, *205*, 151−157.

DOI: 10.1021/acs.jnatprod.5b00321
J. Nat. Prod. XXXX, XXX, XXX−XXX